

# THE INFLUENCE OF THE JAKARTA BAY RECLAMATION ON THE SURROUNDING TIDAL ELEVATION AND TIDAL CURRENT

\*Harman Ajiwibowo<sup>1</sup>, Munawir Bintang Pratama<sup>1</sup>

<sup>1</sup> Faculty of Civil and Environmental Engineering, Institut Teknologi Bandung, Indonesia

\*Corresponding Author, Received: 26 Aug. 2017, Revised: 21 Feb. 2018, Accepted: 20 March 2018

**ABSTRACT:** The Jakarta Bay artificial island reclamation is a part of the spatial arrangement of the Province of DKI Jakarta which is stated in Governor Regulation No. 121/2012. The regulation divides the area into three sub-regions, west, middle and east. In the middle sub-region, the influence of the reclamation of artificial islands, named I, J, K, L and M islands, on the tidal elevation and tidal current is investigated using hydrodynamic modeling with inputs of the river discharges coming into the bay. The plan to build a gate at the southern side of L island is also a part of the study. For normal river discharge, the existence of the reclaimed islands does not influence the tidal elevation significantly, whereas the tidal current is affected by a 200% intensification at a few points. For flood river discharge with a 25-year return period, the tidal elevation is more unstable, with the maximum rising or falling by 2 cm at most locations. The current phase shift is found, and along with the current intensification of round 200%, there is a reduction of the current magnitude. The reclamation and the gate cause some tidal changes, although these are still within the normal range that can accommodate daily activities. The reclamation scenario with the gate is better for the channel at the eastern side of L island since it results in a lower tidal elevation.

*Keywords:* Numerical modeling, Coastal environment, Tidal elevation, Tidal current, Jakarta Bay reclamation.

## 1. INTRODUCTION

The reclamation of Jakarta Bay has been regulated in the Governor Regulation of DKI Jakarta No. 121/2012 for fulfilling the needs for increased space [1]. There will be three sub-regions in the reclamation plan and islands I, J, K, L, and M are in the middle sub-region. This sub-region will provide space for housing, international trading, and offices. To identify environmental risks in the future, studies on the hydrodynamics-related environmental effects of the reclamation are being performed.

In China, relatively more intensive studies have already been carried out to investigate the effect of land reclamation. Xu et al. (2017) developed an integrated modeling framework around the Yellow River Estuary [2]. Peng et al. (2013) studied the total allowable area for coastal reclamation in Xiamen [3]. Feng et al. (2015) used an environmental impact assessment to evaluate the feasibility of some reclamation projects [4].

A study in Jiaozhou Bay was developed by Gao et al. (2014) [5]. There had been a large-scale land reclamation which affected the hydrodynamics and sediment transport in the bay. Gao et al. (2014) set up a three-dimensional barotropic hydrodynamic model based on the Finite Volume Coastal Ocean Model (FVCOM) to investigate changes in tidal dynamic factors in Jiaozhou Bay from 1935 to 2008 [5]. Their next study relating to suspended sediment was developed using FVCOM and UNSW sediment

models [6].

In Jakarta, two studies related to environmental effects on the coast have been carried out to investigate the potential flood [7] and storm surge risk [8]. Meanwhile, Azwar et al. (2013) applied the ecological city theory on a model of sustainable urban infrastructure at the coastal reclamation of North Jakarta using a Structural Equation Model [9].

However, this study aims to investigate the effect of land reclamation in Jakarta Bay on the surrounding tidal parameters. The study uses hydrodynamic modeling to present a comparison of the conditions before and after the construction of the land reclamation. The plan to build a gate at the southern side of L island is also part of the study. A similar study was also presented by Ding et al. (2017), but for port infrastructure [10].

The studies on the tidal parameters are necessary to mitigate any occurrence of water inundation to the land caused by a rise in the tidal elevation, and the occurrence of erosion if the tidal current becomes stronger.

## 2. FIELD SURVEY

The conducted field survey is the bathymetric, tidal elevation, and tidal current surveys. The surveys are performed to acquire the data to be used in the modeling and validation.

## 2.1 Bathymetric Survey

The survey area of about 3300 hectares can be seen in Figs. 1(a) and 1(b). The bathymetric survey documentation is presented in Fig. 2(a). The survey equipment is a Single Beam Echosounder and Odom Hydro truck. The area is located at Jakarta Bay near Indonesia's famous Ancol recreational area.

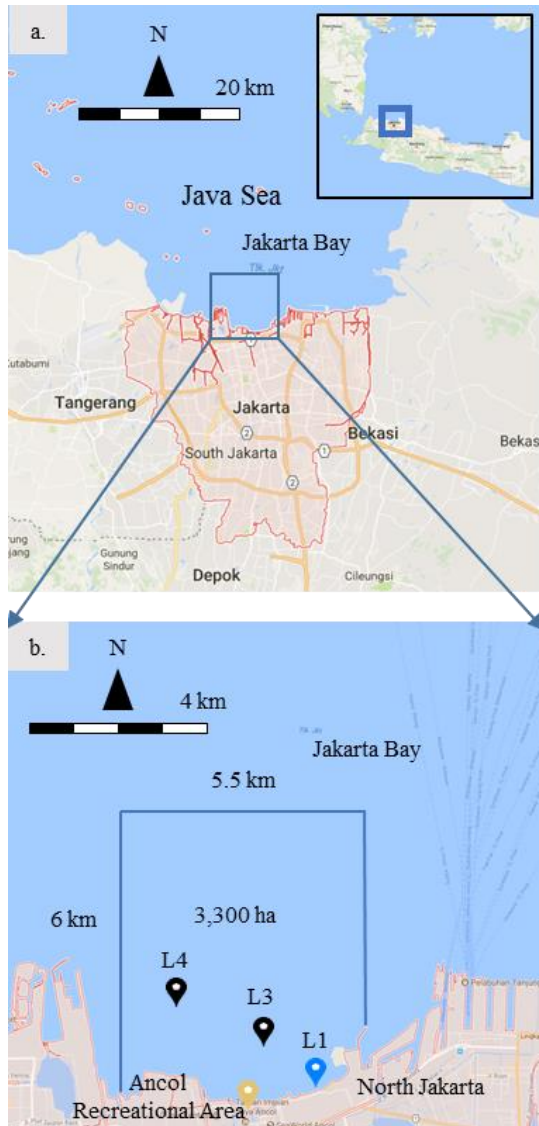


Fig.1 Locations of (a) Jakarta Capital City and (b) the field measurement area (the solid blue box).

## 2.2 Tidal Elevation Field Measurement

The blue pinned mark in Fig. 1(b) denoted as L1 is the location of the tidal elevation field measurement. An Automatic Water Level Recorder was used for the measurement. The result was hourly time series of the water elevation from February 19 to March 6, which is sufficient to present a half-moon cycle. The resulted

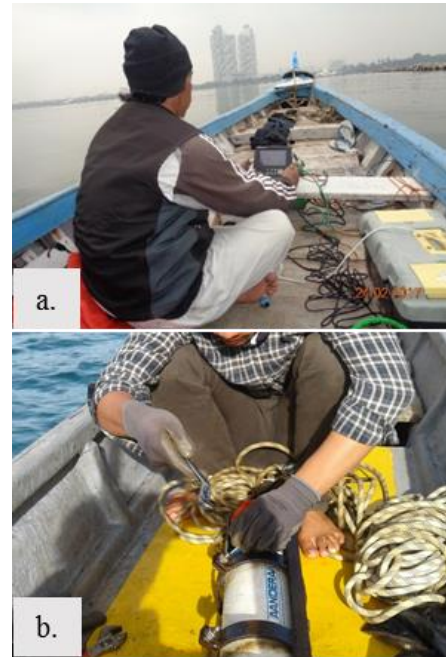


Fig.2 Images of (a) bathymetric survey and (b) the Aanderaa RCM instruments measurement which overlaid with field data [11] is shown in Fig. 3.

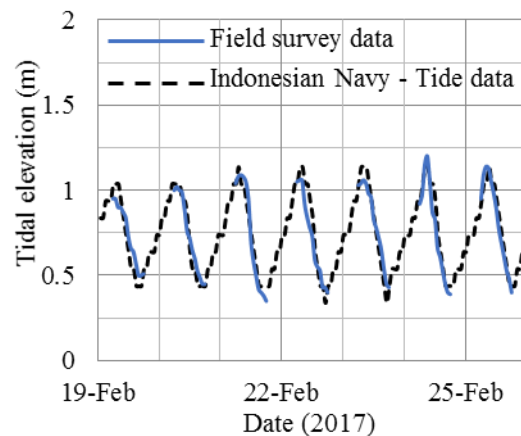


Fig.3 The comparison of the surveyed tidal elevation and secondary data.

## 2.3 Tidal Current Field Measurement

The tidal current field measurement refers to research result by Ajiwibowo et al. (2017) [12]. The two black pins (L3 and L4) in Fig. 1(b) are the locations of the tidal current field measurement. The survey used the Aanderaa RCM Blue (Fig. 2(b)). The current measurements were conducted in 3 water depths, at 0.2d, 0.6d, and 0.8d, where d is the water depth. Each depth measurement was recorded hourly for a period of 24 hours. The depth-averaged of the measured currents are presented in Fig. 4 in the form of a current-rose. Figs. 4(a) and 4(b) are the depth-averaged tidal current at L3 and L4, respectively.

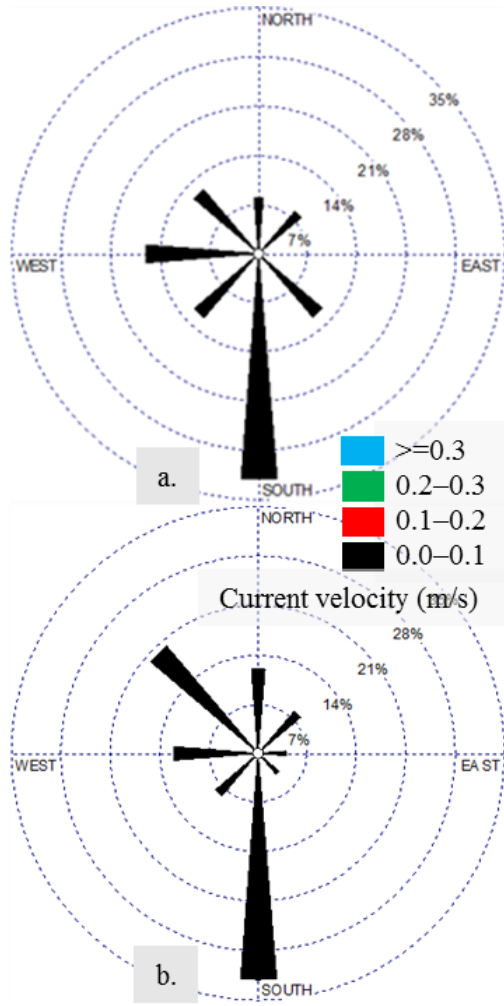


Fig.4 (a) Current-rose of measurement at L3, and (b) at L4 [12]

### 3. NUMERICAL MODEL

A two-dimensional hydrodynamic model was used to simulate the tidal and current pattern distribution at the location of interest. Eq. (1) shows the formula for calculating the model result's accuracy or error ( $\epsilon$ ). The  $\zeta_m$  is the resulted numerical model data and  $\zeta_p$  is the field survey data, and  $\rho$  is the tidal range from field data.

$$\epsilon = \frac{|\zeta_m - \zeta_p|}{\rho} \quad (1)$$

#### 3.1 Governing Equations

RMA2 is a module in the Surface Modeling System (SMS) interface which generates a current pattern resulting from the tidal boundary conditions in the perimeter of the domain, using a two-dimensional finite element method. It is coded by the US Army Corps of Engineers Resource

Development Center.

RMA2 solves the depth-integrated equations of fluid mass (see Eq. (2)) and momentum conservation in two horizontal directions (see Eqs. (3) and (4) for the x and y-axes, respectively) [13]. The governing equations as written in [13] are rewritten as follows:

$$\frac{\partial h}{\partial t} + h \left( \frac{\partial u}{\partial x} + \frac{\partial v}{\partial y} \right) + u \frac{\partial h}{\partial x} + v \frac{\partial h}{\partial y} = 0 \quad (2)$$

$$h \frac{\partial u}{\partial t} + hu \frac{\partial u}{\partial x} + hv \frac{\partial u}{\partial y} - \frac{h}{\rho} \left[ E_{xx} \frac{\partial^2 u}{\partial x^2} + E_{xy} \frac{\partial^2 u}{\partial y^2} \right] + gh \left[ \frac{\partial a}{\partial x} + \frac{\partial h}{\partial x} \right] + \frac{gun^2}{\left( 1.486h^{1/6} \right)^2} (u^2 + v^2)^{1/2}$$

$$-\zeta V_a^2 \cos \psi - 2hv\omega \sin \Phi = 0 \quad (3)$$

$$h \frac{\partial v}{\partial t} + hu \frac{\partial v}{\partial x} + hv \frac{\partial v}{\partial y} - \frac{h}{\rho} \left[ E_{yx} \frac{\partial^2 v}{\partial x^2} + E_{yy} \frac{\partial^2 v}{\partial y^2} \right] + gh \left[ \frac{\partial a}{\partial y} + \frac{\partial h}{\partial y} \right] + \frac{gvn^2}{\left( 1.486h^{1/6} \right)^2} (u^2 + v^2)^{1/2}$$

$$-\zeta V_a^2 \sin \psi + 2hu\omega \sin \Phi = 0 \quad (4)$$

where  $h$  is the water depth,  $x$  and  $y$  are the Cartesian coordinates,  $t$  is time,  $u$  and  $v$  are the velocities in Cartesian coordinates,  $\rho$  is the fluid density,  $E$  is the eddy viscosity coefficient,  $g$  is the acceleration due to gravity,  $a$  is the elevation of the bottom,  $n$  is the Manning's roughness  $n$ -value, 1.486 provides the conversion from SI to non-SI units,  $\zeta$  is the empirical wind shear coefficient,  $V_a$  is the wind speed,  $\psi$  is the wind direction,  $\omega$  is the rate of angular rotation of the Earth, and  $\Phi$  is the local latitude [13].

#### 3.2 Model Setup

The influence of the artificial islands and the existence of the gate is investigated using hydrodynamic modeling. The model setup refers to previous research result done by Ajiwibowo et al. (2017) [12]. Fig. 5 shows the scenarios domain of the numerical model in this study at Jakarta Bay. The existing conditions, also called the existing scenario domain, are presented in Fig. 5(a). This scenario does not include any artificial islands, while Fig. 5(b) shows the domain of scenarios A and B, including the islands. The difference between these scenarios is the presence of a gate on the south side of L island in Scenario B.

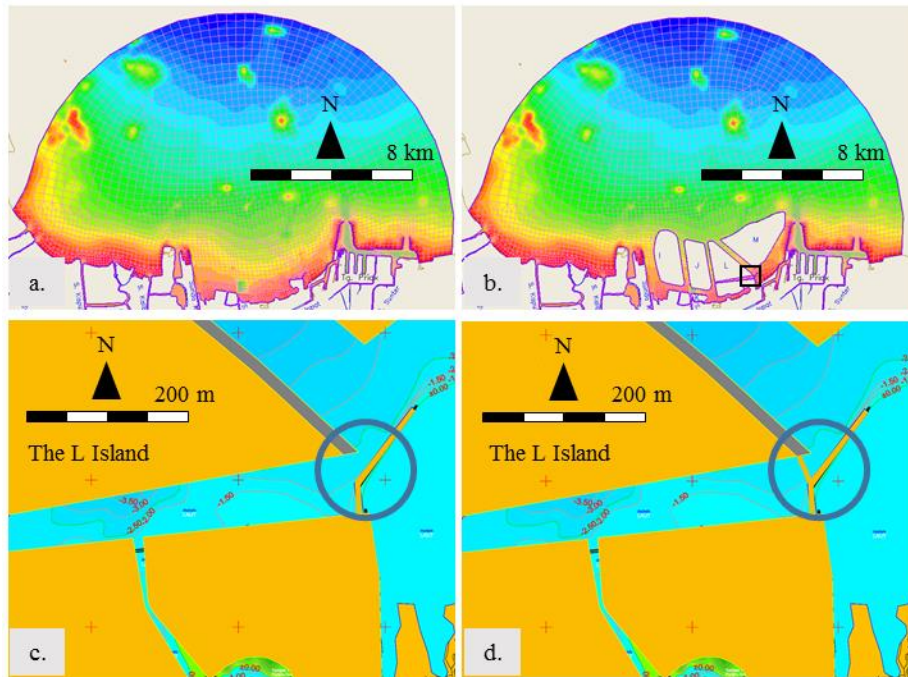


Fig.5 (a) Domain of existing condition, (b) future scenario. Enlarged view of the south side of L island: (c) scenario A without gate, and (d) scenario B with gate [12]

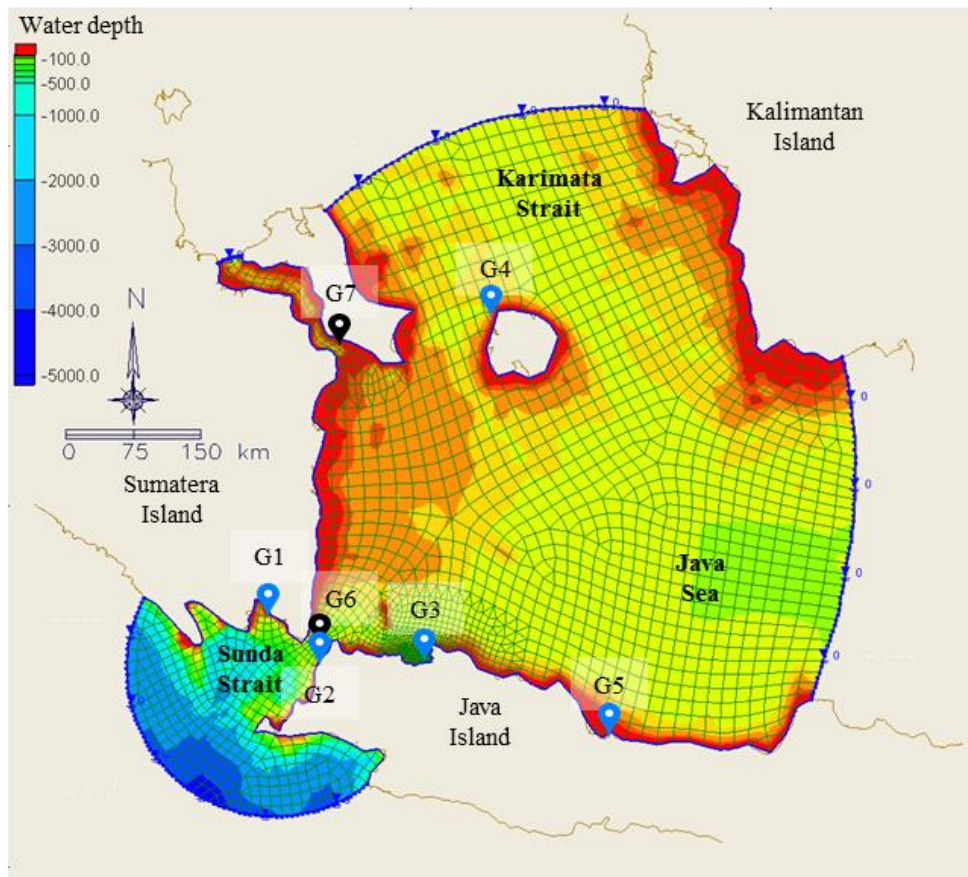


Fig.6 The domain of the global model, covering Java Sea, Karimata Strait, and Sunda Strait. The blue and black pins show the tidal elevation and tidal current validation data [12]

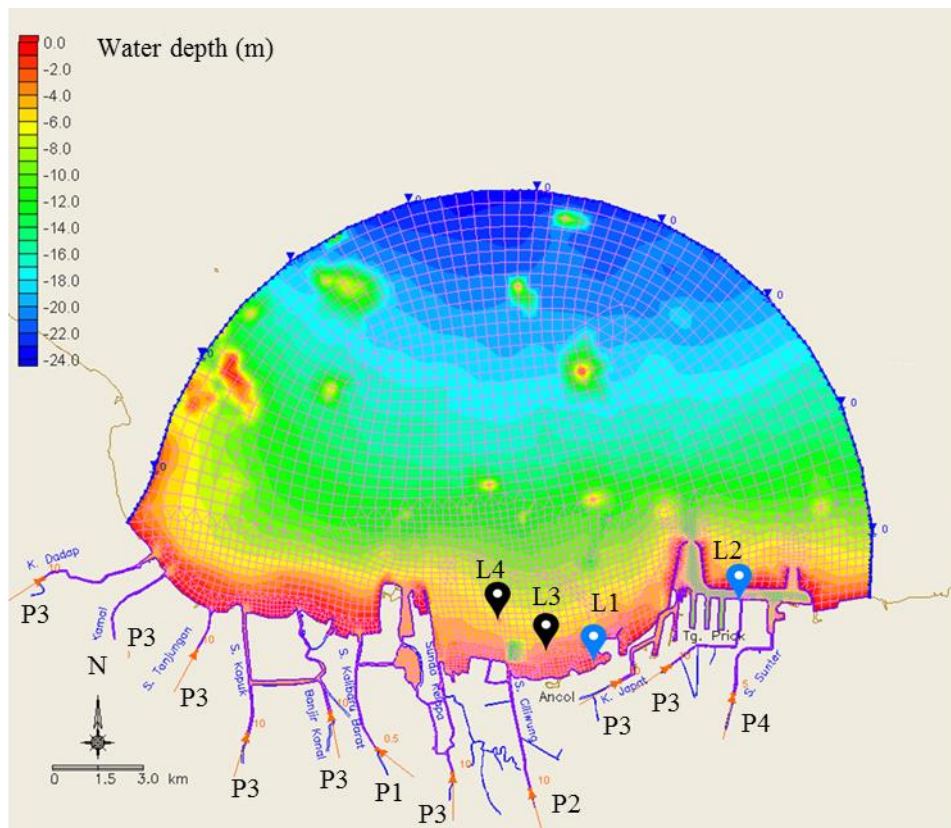


Fig.7 The domain of the local model covering the area of interest in Jakarta Bay. The blue and black pins show the tidal elevation and tidal current validation data [12].

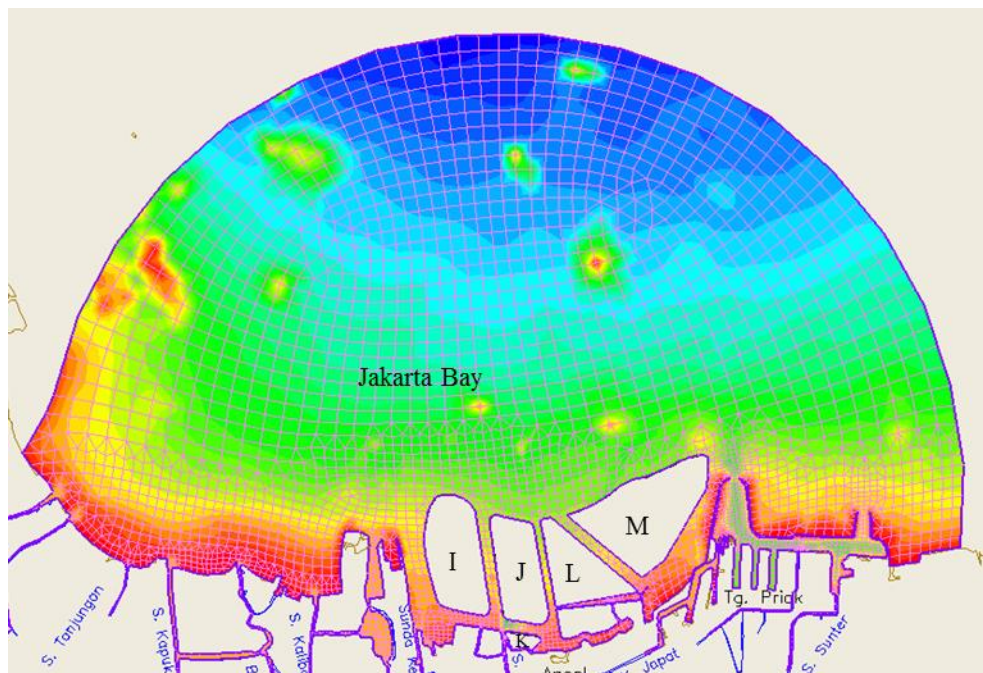


Fig.8 The domain of the scenarios model, including the existence of artificial islands. Scenario B includes a gate in the south channel of L island, Scenario A without [12].

There are three stages in the numerical modeling, the global, local, and scenario models. The global model domain covers Java Sea, Karimata Strait, and Sunda Strait as shown in Fig. 6. The boundary conditions are generated using NaoTide [14]. The global model results in a sea surface elevation and tidal currents, and both are validated with field data from Indonesia Navy Tide Databases [11], [15].

The second stage is the local model which covers a smaller area around Ancol recreational area in Jakarta Bay as shown in Fig. 7. There are additional important inputs in the local model, which is the volumes of water coming into the bay from the three rivers, the Grogol, Ciliwung and Sunter Rivers. The model's purpose is to produce a specific hydrodynamic model at the bay forced by tidal and river discharges. The local model result is validated with tidal elevation (L1 and L2) and tidal current data (L3 and L4) from the field survey and Indonesia Navy Tide Databases [11], [15].

After being validated, the local model is then modified into the scenarios model by modifying the bathymetry to represent the artificial islands, I, J, K, L, and M, as well as the gate, as shown in Fig. 8.

Unlike the global model, the local and scenarios models include river discharges since the river system significantly affects the water circulation in Jakarta Bay. The three main rivers are shown in Fig. 9, Grogol, Ciliwung, and Sunter Rivers, are denoted as R1, R2, and R3, respectively. The normal/monthly ( $S_N$ ) and 25-year return period flood river discharges ( $S_{25}$ ) of the main rivers are given in Table 1. However, there are other tributaries of small rivers which also flow into Jakarta Bay. These small river discharges are taken as a proportion of the main river discharges, as set out in Table 2. The rivers and their discharge values are shown in Fig. 7.



Fig.9 Location of main rivers in Jakarta Capital City

### 3.3 Global Model Validation

The validations of the global model are the validation of tidal-induced sea surface elevation and tidal-induced current magnitudes taken from the Indonesia Navy Tide Database. The elevation validation was carried out at 5 locations along the Java Sea, Karimata Strait, and Sunda Strait denoted as G1 to G5 in Fig. 6. While the current velocity is validated at G6 and G7 in Fig. 6. The results of the validations are presented in Table 3, which shows a good agreement.

Table 1 Monthly and flood discharge of main rivers

	Discharge (m <sup>3</sup> /s)			
	Grogol R1	Ciliwung R2	Sunter R3	
Jan.	1.2	48.4	10.1	
Feb.	1.5	51.5	12.4	
Mar.	1.2	38.6	11.9	
Apr.	1.1	33.7	11.2	
May	1.0	32.9	10.4	
Month ( $S_N$ )	0.8	25.9	8.5	
Jul.	0.8	22.5	7.4	
Aug.	0.8	19.3	6.5	
Sept.	0.9	24.7	6.4	
Oct.	1.0	27.3	7.2	
Nov.	1.5	35.0	8.7	
Dec.	0.9	32.7	9.1	
Return period ( $S_{25}$ )	25 years	411.25	886.4	295.5

Table 2 The other small river discharges proportional to main river discharges

Unit discharge	Equivalent discharge
P1	R1
P2	R2
P3	1/3 R2
P4	R3

Table 3 Errors in tidal-induced surface elevation and tidal-induced current validation of the global model

Site	Site	Error (%)
G1	Panjang	3.7
G2	Ciwandan	9.8
G3	Tanjung Priok	6.5
G4	Tanjung Pandan	5
G5	Cirebon	9.1
G6	Sunda Strait	7.9
G7	Nemesis Shoal	5.8

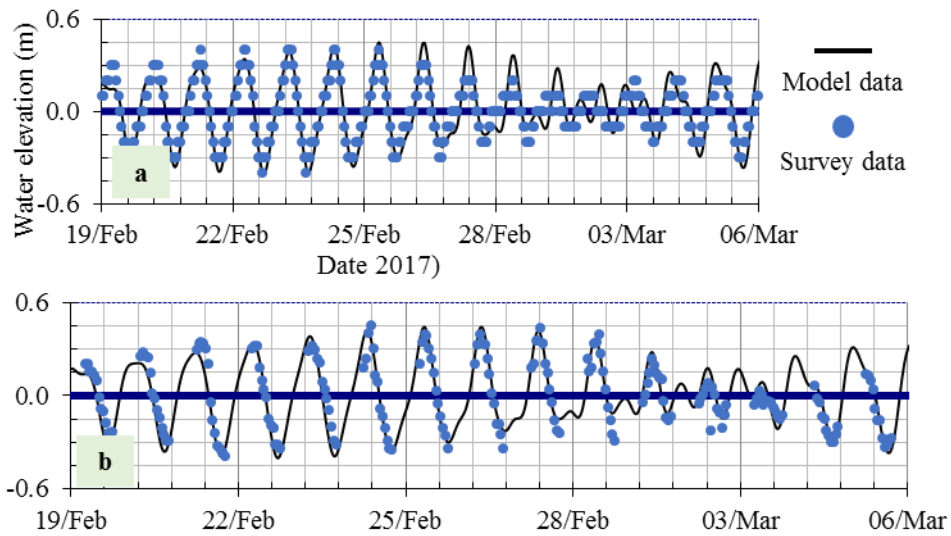


Fig. 10 Results of local model tidal elevation validation, at (a) Tanjung Priok Station L2 and (b) field measurement location L1

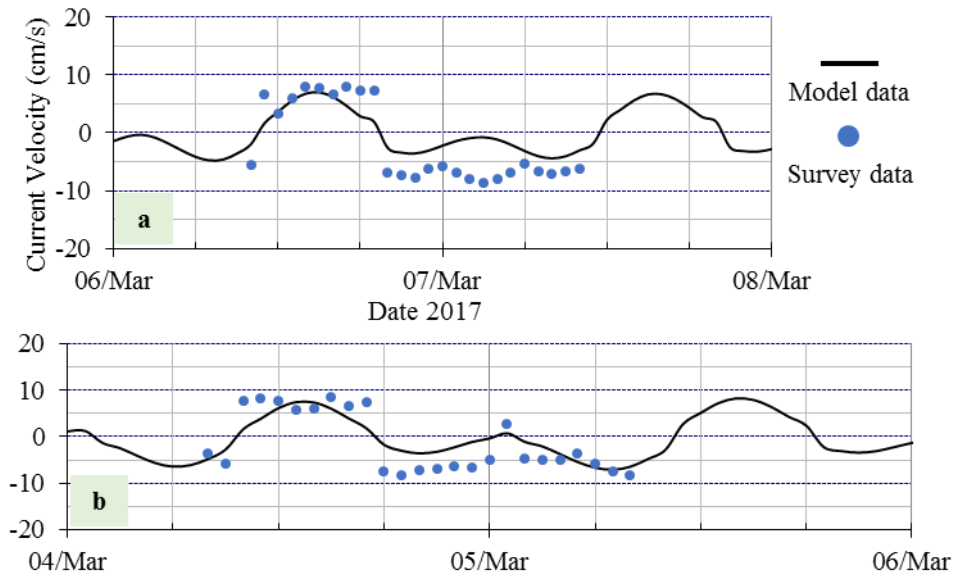


Fig.11 Results of local model tidal current validation, at field measurement locations (a) L3 and (b) L4

### 3.4 Local Model Validation

The local model is validated in the parameters of tidal elevation and tidal current. The comparison data is obtained from field measurement and the Indonesia Navy Tide Database. The location of the tidal-induced sea surface elevation validation is shown in Fig. 7, marked as L1 and L2. For the tidal-induced current magnitudes, the validation locations are marked as L3 and L4. The results of validation are given in Figs. 10 (The average errors are 6.5%) and 11 for the tidal elevation and tidal current. The validations present acceptable errors, meaning that the local model is reliable, and can be used as the basis of the scenarios model.

### 4. ANALYSIS

This analysis uses the resulting scenarios model to assess the change of the tidal elevation and the tidal current due to the artificial land reclamation and gate placement. The influences of normal and 25-year flood river discharges are also observed. Fig. 12 shows the locations of the cross-sections and points to be observed.

For the investigated cross-sections and points are given in Fig. 12, three sections are denoted as A1–A2, B1–B2, and C1–C2. The subscripts 1 and 2 indicate the start and end of the section, respectively. The sections A1–A2, B1–B2, and C1–C2 show the change in elevation along the coastal

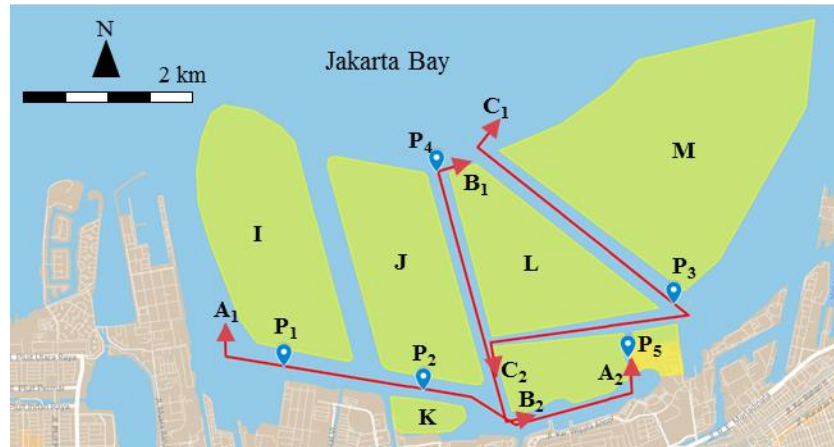


Fig.12 The investigated cross-sections and points

area, at the south side of L island, and at both the east and west sides of L island, respectively.

Five points, denoted by P1 to P5, are defined. P1 and P2 show the change in the current along the coast. P3, P4, and P5 show the change in the current around L island. The impact of the existence of the gate will be presented by section C1-C2 and both section P3 and section P5.

#### 4.1 The Influence on Tidal Elevation

The impact of the artificial islands and the existence of the gate in the area of interest on the tidal elevation is investigated around L island. Fig. 13 compares the existing and scenarios model results. Figs. 13(a) to 13(c) present the comparison of the tidal elevation change when the gate is not present, i.e. scenario A, while Fig. 13(d) to 13(f) present the condition when the gate exists, i.e. scenario B.

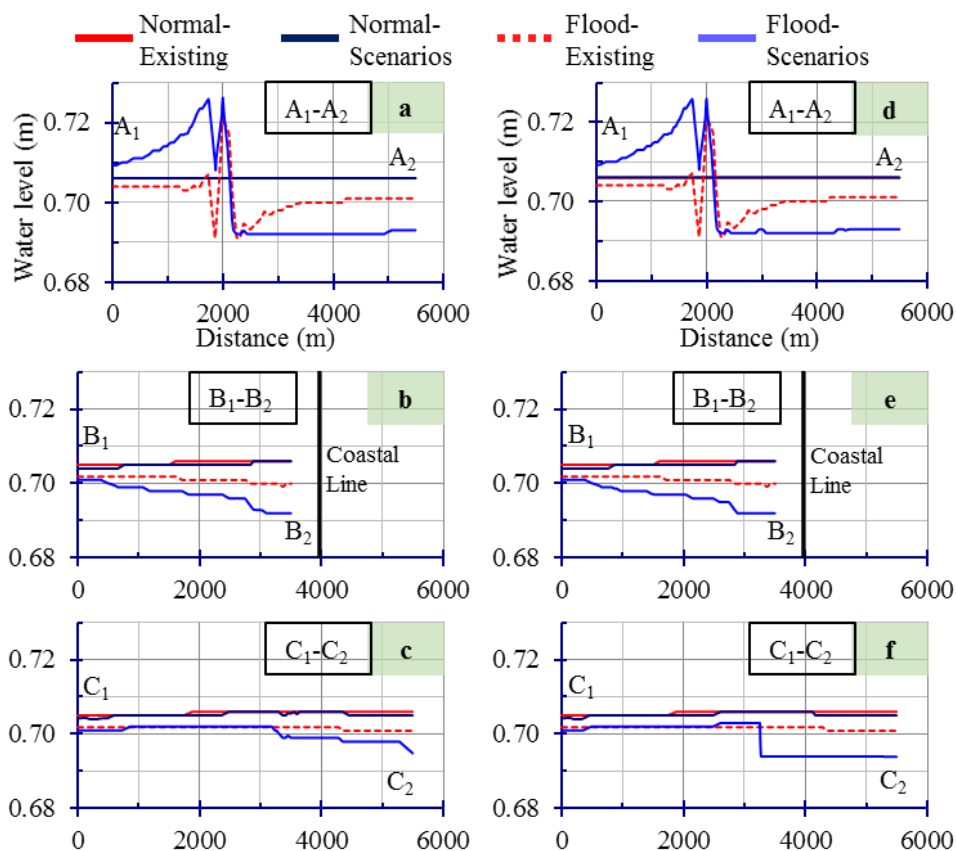


Fig.13 Comparison of the tidal elevation change between the existing and scenarios model, (a-c) for scenario A and (d-f) for scenario B, in monthly and flood discharges.

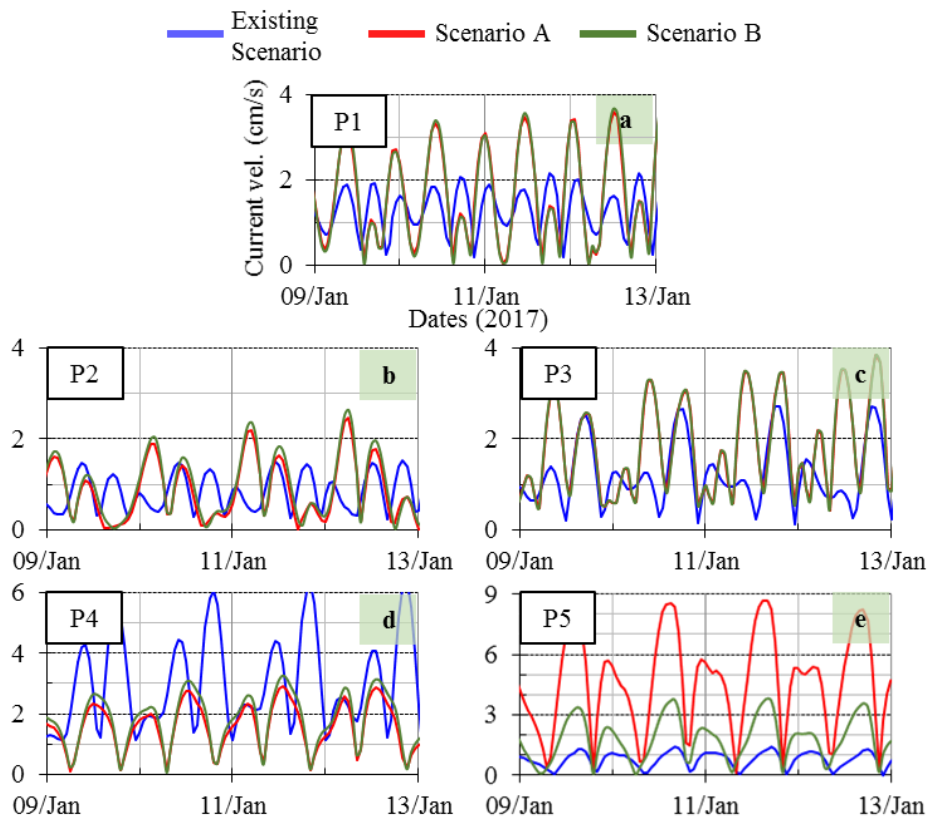


Fig.14 Comparison of the tidal current change between the existing and scenarios model for monthly discharge

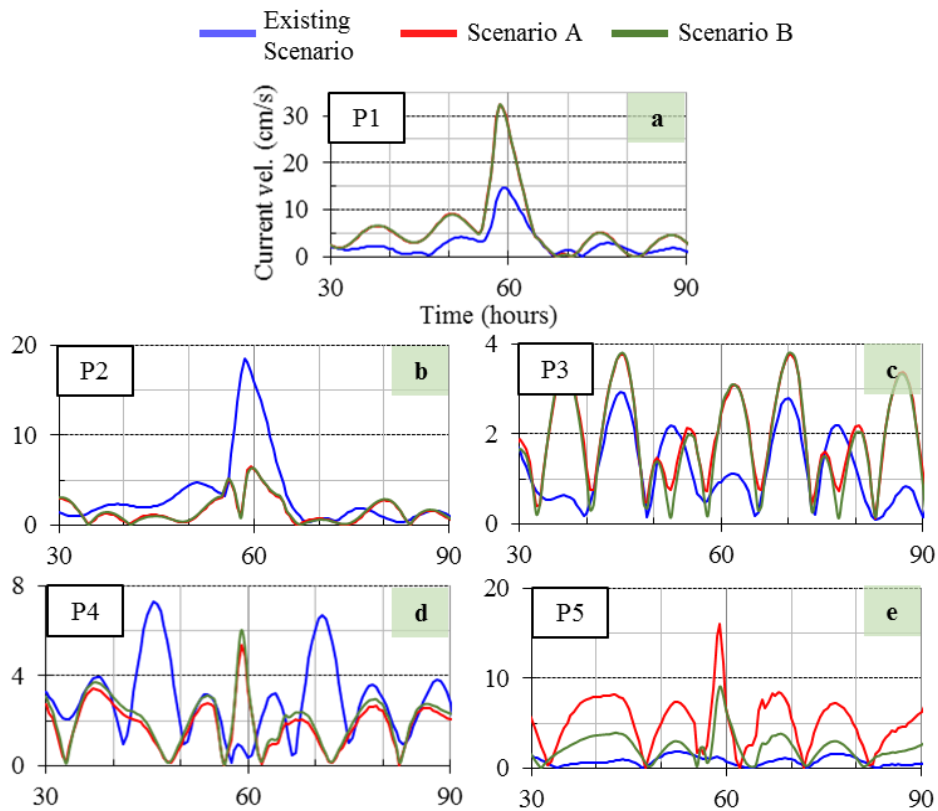


Fig.15 Comparison of the tidal current change between the existing and scenarios model for flood (25-year return period) discharge

The gate, whether open or closed, does not affect the tidal elevation much. The flood discharge causes a more unstable tidal elevation according to all comparisons. In cross-section A1–A2, the results of the comparison clearly indicate the tidal elevation difference (almost 2 cm at most) between the existing model and the scenario model.

#### **4.2 The Influence of the Tidal Current**

The changes of tidal-induced current are observed along the North Jakarta coast at five locations as shown in Fig. 12. Figs. 14(a) to 14(e) show the velocity during normal river discharges, while Figs. 15(a) to 15(e) show the velocity during the 25-year river flood discharge.

In both scenarios, the reclamation presents a clear influence on the tidal current (under normal discharge) at the observed points. For normal river discharges input, the existence of the reclamations causes an increase of about 2 cm/s at wider channel openings such as point P1, since the channel opening in P1 is wider than in P4. Most of the water mass passes through wider channels rather than smaller channels, so the velocity at P4 decreases to about 4 cm/s during peak current.

As for the flooded river discharge input, the water mass will tend to pass through wider channels rather than smaller channels. The amplitude of the tidal current at peak time increases by around 100% at P1, as much as 17.5 cm/s (see Fig. 15(a)). For some smaller channels as in Fig. 15(b) and 15(d), the peak decreases to 30%. The presence of the gate does not have much influence on the hydrodynamic change, except for the small channel at point P5, where the water mass tends to flow to the east side of L island when the gate is open, with a velocity up to 8.5 cm/s at P5.

#### **5. CONCLUSION**

The study includes the field measurement, numerical modeling, and model analysis. The surveyed tidal elevation resulted in a good agreement with the secondary data, as shown in Fig. 3 [11]. The tidal range is 104.52 cm with a diurnal tide type. And the result of tidal current survey presents that the currents are mainly directed to the south and the magnitudes are mostly in the range of 0–0.1 m/s, see Fig. 4.

The numerical hydrodynamic model of the global and local models in this study presents a good agreement with field measurement data and secondary data from the Indonesian Navy table. The average errors are about 7%.

Under normal discharge, the reclamation of islands does not influence the tidal elevation significantly. The tidal elevation at the three investigated cross-sections changes by only a few

millimeters. The tidal current increases by 100% at the south side of the island I and at the south side gap of L island.

Under flood discharge with a 25-year return period, the tidal elevation in the scenarios model is more unstable with a maximum 2 cm ascent or descent at most locations, as found at all of the observed cross-sections. A current phase shift is also observed, as well as a current intensification and reduction of around 100%.

The reclamation results in small tidal changes, so do the existence of the gate. The reclamation scenario with the gate is better for defending the channel at the east side of L island since it results in a lower tidal elevation. This work is very promising for further studies, such as to investigate the sediment transport, seabed change, and even checking the environmental feasibility of a planned giant sea wall at a larger scale.

#### **6. ACKNOWLEDGMENTS**

The authors would like to present a big appreciation and gratitude to PT Pembangunan Jaya Ancol for supporting and sponsoring this research.

#### **7. REFERENCES**

- [1] Governor of DKI Jakarta, Penataan Ruang Kawasan Reklamasi Pantai Utara Jakarta. Governor Regulation of DKI Jakarta Province No. 121 Year 2012.
- [2] Xu Y., Cai Y., Sun T., Tan Q., A Multi-Scale Integrated Modeling Framework to Measure Comprehensive Impact of Coastal Reclamation Activities in Yellow River Estuary, China. *Marine Pollution Bulletin*, Vol. 122, 2017, pp. 27–37.
- [3] Peng B., Lin C., Jin D., Rao H., Jiang Y., Liu Yan, Modeling the Total Allowable Area for Coastal Reclamation: A Case Study of Xiamen, China. *Ocean & Coastal Management*, Vol. 76, 2013, pp. 38–44.
- [4] Feng L., He J., Ai J., Sun X., Bian F., Zhu X., Evaluation for Coastal Reclamation Feasibility Using a Comprehensive Hydrodynamic Framework: A Case Study in Haizhou Bay. *Marine Pollution Bulletin*, Vol. 1, 2015, pp. 182–190.
- [5] Gao G.D., Wang X.H., Bao X.B., Land Reclamation and Its Impact on Tidal Dynamics in Jiaozhou Bay, Qingdao, China. *Estuarine, Coastal, and Shelf Science*, Vol. 151, 2014, pp. 285–294.
- [6] Gao G.D., Wang X.H., Bao X.W., Song D., Lin X.P., Qiao L.L., The Impacts of Land Reclamation on Suspended-Sediment Dynamics in Jiaozhou Bay, Qingdao, China. *Estuarine, Coastal and Shelf Science*, in the press- corrected proof, 2017.
- [7] Takagi H., Esteban M., Mikami T., Fujii D, Projection of Coastal Floods in 2050 Jakarta. *Urban Climate*, Vol. 17, 2016, pp. 135–145.

- [8] Esteban M., Takagi H., Mikami T., Aprilia A., Fujii D., Kurobe S., Utama N.A., Awareness of Coastal Floods in Impoverished Subsiding Coastal Communities in Jakarta: Tsunamis, Typhoon Storm Surges and Dyke-Induced Tsunamis. *International Journal of Disaster Risk Reduction*, Vol. 23, 2017, pp. 70–79.
- [9] Ding P., Guo W., Wang X.H., Ge J., Song D., A system shift in tidal choking due to the construction of Yangshan Harbour, Shanghai, China. *Estuarine, Coastal and Shelf Science*, in press-corrected proof, 2017.
- [10] Azwar S.A., Suganda E., Tijptoherijanto P., Rahmayanti H., Model of Sustainable Urban Infrastructure at Coastal Reclamation of North Jakarta. *Procedia Environmental Sciences*, Vol. 17, 2013, pp. 452–461.
- [11] Tide Tables of Indonesia. Indonesia: Dinas Hidro-Oseanografi TNI-AL, 2017, ch. 31. pp. 221–227.
- [12] Ajiwibowo, H., Pratama, M.B., The Effect of Gate Existence at L Island on The Seabed Profile Due to Reclamation of Jakarta Bay, *International Journal of Engineering and Technology*, Vol. 9, 2017, pp. 3763-3774
- [13] User Guide to RMA2 WES Version 4.5. USA: US Army, Engineer Research and Development Center, Waterways Experiment Station, Coastal and Hydraulic Laboratory, 2005, ch. 2. pp. 4–6.
- [14] Matsumoto K., Takanezawa T., Ooe M., Ocean Tide Models Developed by Assimilating TOPEX/POSEIDON Altimeter Data into Hydrodynamical Model: A Global Model and a Regional Model around Japan. *Journal of Oceanography*, Vol. 56, 2000, pp. 567–81.
- [15] Tidal Stream Tables of Indonesia Archipelago. Indonesia: Dinas Hidro-Oseanografi TNI-AL: 2017, ch. 11. pp 79–85.

---

Copyright © Int. J. of GEOMATE. All rights reserved, including the making of copies unless permission is obtained from the copyright proprietors.

---